ABSOLUTE RADIOMETRIC CALIBRATION OF DIGITAL IMAGING SYSTEMS

Steven W. Brown, Thomas C. Larason, Catherine Habauzit, George P. Eppeldauer,
Yoshihiro Ohno, and Keith R. Lykke
National Institute of Standards and Technology, Gaithersburg, MD 20899

ABSTRACT

We have developed a tunable laser-based facility for the absolute radiometric calibration of digital imaging systems such as CCD cameras, spectrographs, and microscopes. Several types of silicon-based digital imaging systems have been calibrated in this new facility, including a commercially available camera equipped with a removable photopic filter, a custom-designed digital microscope, and a CCD spectrograph. We present results of the CCD camera calibration in detail and discuss relevant aspects of the microscope and spectrograph calibrations. During the radiometric calibration, the pixel-to-pixel uniformity, linearity, and absolute spectral responsivity of each system were determined over the visible spectral range (400 nm to 800 nm). Each of these aspects of the CCD camera calibration will be presented, along with a discussion of the measurement uncertainties.

Keywords: calibration, CCD, digital camera, radiometry

1. INTRODUCTION

Improvements in the operation and performance of Digital Imaging Systems (DIS's) have led to an explosion in the use of these systems in a variety of scientific, medical, and industrial imaging applications. In many of these new applications, it is important that the spectral characteristics of the imaging system as well as its spatial (geometric) properties be well characterized and its photometric, radiometric, or colorimetric performance known. This has resulted in increased demand for characterization and calibration methodologies that are traceable to common standards.

By knowing the spectral responsivity of a DIS, one can accurately predict its performance under differing operating conditions. Currently, these systems can be calibrated with relative combined standard uncertainties of approximately 5 % to 10 %. In many cases, DIS's are calibrated against broad-band incandescent sources – such as Illuminant A – and subsequently measure sources with very different spectral power distributions. In this case, the measurement uncertainties are not well known in general, and can be much larger than expected.

2. DESCRIPTION OF THE SIRCUS FACILITY

We have developed a facility at the National Institute of Standards and Technology (NIST) for Spectral Irradiance and Radiance Responsivity Calibrations using Uniform Sources (SIRCUS) to calibrate DIS's. In this facility — shown in Fig 1 — lasers are directed into an integrating sphere to produce a monochromatic, Lambertian source for irradiance and radiance responsivity calibrations. This integrating sphere source (ISS) has been used to calibrate the spectral radiance and irradiance responsivity of a variety of detectors and imaging systems [1]. The two critical cornerstones of the facility are broadly tunable continuous-wave (cw) laser sources and reference standard detectors that are well-characterized and calibrated with low uncertainties to determine the radiance of the ISS with low uncertainty.

A variety of lasers are used to provide continuous coverage over the spectral range from 370 nm to 1000 nm. A Ti:sapphire laser provides tunable coverage from 690 nm to 1000 nm, frequency-doubling enables tunability from 370 nm to 450 nm. Discrete lasers were used for the spectral range from 450 nm to 550 nm and dye lasers are used to cover the spectral region from 550 nm to 700 nm. Currently, dye lasers are used to cover the spectral range from 415 nm to 700 nm.

Reference standard detectors with spectral power responsivities directly traceable to the NIST primary standard equipped with precision apertures were used to determine the sphere radiance [2]. These trap detectors are calibrated for spectral power responsivity directly against a cryogenic radiometer over the spectral range from 405 nm to 920 nm [3]. From the power responsivity and the aperture area, the irradiance responsivity of the trap detector is determined. By measuring the distance between the sphere exit port and the trap detector entrance aperture and the area of the ISS exit port, the radiance of

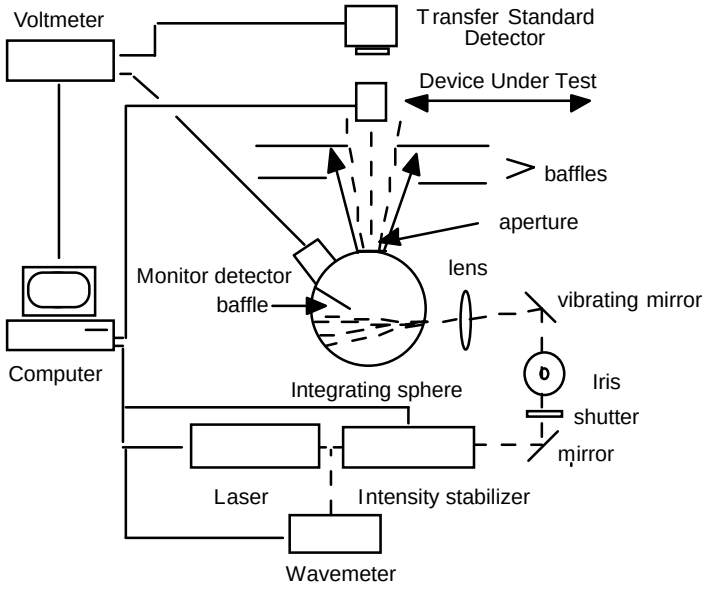

Fig. 1. Schematic diagram of the SIRCUS facility.

the ISS was determined with a relative combined standard uncertainty of 0.1 % [4, 5]. A silicon monitor detector mounted on the wall of the ISS was used to correct for small power fluctuations in the laser between measurements with the reference standard detector and the DIS.

3. CALIBRATION RESULTS

In general, the absolute spectral responsivity (ASR) of an instrument, $R(\lambda)$, relates the signal measured by a detector, S, to the spectral radiance of the source being measured, $L(\lambda)$:

$$S = \int R(\lambda)L(\lambda)\,d\lambda\,. \qquad (1)$$

The integration is over the full spectral bandwidth of the source. A DIS can be considered to be comprised of i by j independent detectors, with an individual measurement equation for each detector, or pixel, in the array. Each pixel in the array will also image a different area of the ISS, and in general:

$$S_{i,j} = \int R_{i,j}(\lambda)L_{i,j}(\lambda)\,d\lambda\,, \qquad (2)$$

with i defining the column position and j equal to the corresponding row in the array. $L_{i,j}(\lambda)$ refers to the radiance of the spatial region of the sphere exit port imaged onto pixel i, j. Note that for uniform sources, we can eliminate the spatial dependence on radiance: $L_{i,j}(\lambda) \sim L(\lambda)$.

Because we are using narrow-band laser sources (with a bandwidth of approximately 10 MHz, or 0.00001 nm), $L(\lambda)$ can be approximated by a delta function, $L(\lambda)=L(\lambda_o)\delta(\lambda - \lambda_o)$, and Eq. 2 can be rewritten as,

$$S_{i,j} = R_{i,j}(\lambda_o)L(\lambda_o)\,. \qquad (3)$$

Knowing the source radiance $L(\lambda_o)$ and measuring the CCD signal $S(\lambda_o)$, we obtain a direct measurement of the desired quantity $R_{i,j}(\lambda_o)$:

$$R_{i,j}(\lambda_o) = S_{i,j} \big/ L(\lambda_o)\,. \qquad (4)$$

By tuning the wavelength of the calibration source, we directly obtain the absolute spectral responsivity of each element in the DIS.

To complete the radiometric calibration of an instrument, other factors need to be considered as well, including the linearity of the response and the exposure time correction.

3.1. Camera Calibration

We calibrated an 8-bit silicon-based CCD camera with 640 x 480 pixels equipped with a 35 mm focal length lens and a removable photopic filter. The instrument field-of-view under normal operating conditions is 13.5°. It comes equipped with 8 user-selectable shutter speeds, enabling measurements of luminance levels as low as 0.34 cd/m^2. It has a short-term repeatability of 0.4 %, and is calibrated by the manufacturer against Illuminant A with a stated relative combined standard uncertainty (k=1) of 4 %. The camera pixel-to-pixel response uniformity, linearity, and absolute responsivity — both with and without the photopic V(λ) filter on the front of the camera — were determined.

We used a 20 cm diameter Spectralon-coated integrating sphere with a 5.34 cm diameter exit port to calibrate the CCD camera. Typical power levels of radiation introduced into the ISS range from a few mW to a few hundred mW, depending on the laser used, giving a source radiance in the range from 1 x 10^{-7} W/mm^2/sr to 1 x 10^{-4} W/mm^2/sr. Prior to determining the responsivity of the CCD camera, the monitor detector was calibrated against the reference standard detector over the

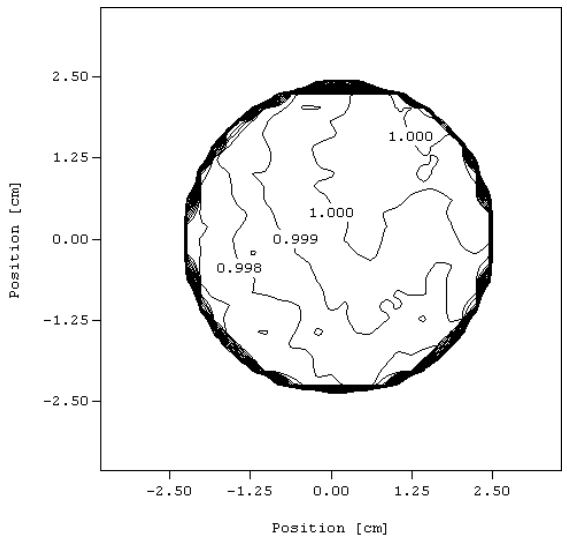

Fig. 2. ISS exit port radiance uniformity with 532 nm excitation.

wavelength range of interest. The calibration related the monitor detector signal to the ISS radiance. The CCD camera was then aligned in front of the ISS and its radiance responsivity determined. During the camera calibration, the sphere radiance was determined at a particular wavelength by measuring the monitor detector signal.

We measured the uniformity of the ISS at 488 nm, 532 nm, and 633 nm using a temperature-stabilized Si radiometer with a narrow field of view mounted on a computer controlled two-axis (XY) translation stage. The stage was stepped in 2 mm increments over a 6 cm by 6 cm square area (an area larger than the area of the sphere exit port). The radiometer signal, normalized by the sphere monitor photodiode signal, was recorded at each position. Results are shown in Fig. 2 for the relative radiance over the ISS exit port at 532 nm; the 633 nm and 488 nm results were similar. As shown in the figure, the radiance from upper right quadrant of the sphere is slightly larger than the radiance from the rest of the sphere. We therefore allow $L_{i,j}(\lambda) \approx L(\lambda)$, with an added relative standard uncertainty of 0.25 %.

We then positioned the camera in front of the ISS exit port. Using a target grid centered on the ISS exit port, we positioned the camera to image the central 4 cm by 3 cm region of the sphere exit port. Prior to determining the absolute responsivity of the CCD, it is necessary to measure and correct for any non-linearity in the response of the camera. We therefore measured the response of the CCD array, averaged over the central 50 by 50 pixels, as the sphere radiance was changed. The measurements involved changing the intensity of the laser light entering the ISS (by adjusting the throughput of a laser power controller) and comparing the radiance of the sphere measured by the CCD with the known ISS radiance determined by the calibrated monitor photodiode. The 8-bit camera has a maximum digital number (DN) of 255, corresponding to a 90 % of the CCD full-well capacity; data were taken with the same CCD exposure time (2 ms) over a radiance range giving count levels varying from approximately 10 DN to 240 DN. The resultant data are plotted in Fig. 3 as the ratio of the CCD signal to the sphere radiance versus the CCD signal (DN). If the CCD response were linear, the ratio of the CCD signal to the ISS radiance would remain constant as a function of CCD count level. However, the ratio increased sharply as the CCD camera signal increased from 10 DN to 100 DN. Above 100 DN, the ratio continued to rise slightly, increasing from a value of approximately 60 at 100 DN to a value of approximately 63 at 230 DN. In determining the absolute radiance responsivity of the CCD, we normalized individual data sets to the high-count level, with the individual scaling factors determined by the results shown in Fig. 3.

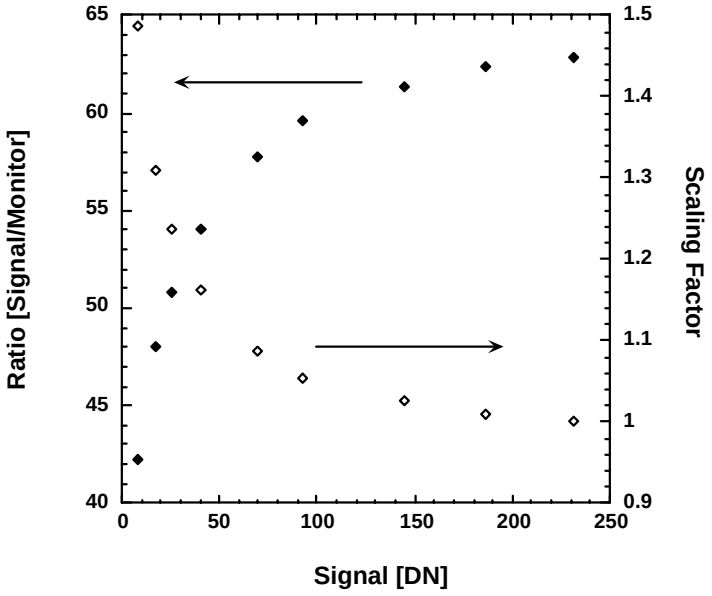

Fig. 3. Non-linear response of the CCD camera and the resultant scaling factors used in the absolute responsivity calibration.

Note that we only calibrated the linearity of the CCD using a shutter setting corresponding to an exposure time of 2 ms. It is difficult to distinguish between a non-linearity in the CCD response, and a variability in the camera readout offset value. For example, we

performed a correction to the response of the CCD by changing the offset level by 7 DN. Applying this simple correction to the data in Fig. 3, the response of the CCD camera was linear to within 1 % over the range from 25 DN to 230 DN.

The CCD camera was then positioned in front of the ISS, and its spectral responsivity, in DN per second per unit radiance, was determined. During the calibration on SIRCUS, the laser was tuned to the wavelength of interest. The CCD camera measured the radiance from the ISS exit port and the radiance responsivity (DN/s/(W/cm^2/sr)) was calculated by dividing the CCD output signal, corrected for the exposure time, by the sphere radiance. During the calibration, images were acquired with several different exposure times. The CCD responsivity was measured for different exposure times at several wavelengths during the calibration. The CCD responsivity agreed to within 1 % for the different exposure times.

The pixel-to-pixel responsivity of the camera was uniform over the central 90 % of the array to within approximately 5 %, as shown in Fig. 4(a) for 580 nm excitation. With the photopic filter installed, the non-uniformity in the CCD responsivity increased to approximately 10 %, as shown in Fig. 4(b). All measurements were performed under the same conditions. The data were not corrected for the non-uniformity of the ISS radiance because it was negligible compared with the non-uniformity of the pixel-to-pixel responsivity of the CCD.

To determine the ASR, we averaged the response of the central 50 by 50 pixels over the wavelength range from 400 nm to 800 nm. At the time of the calibration, we did not have continuously tunable lasers for the spectral range from 450 nm to 550 nm. To fill in this spectral region, we calculated the relative responsivity using the output from a lamp-monochromator source (4 nm bandwidth) [6], and determined the absolute responsivity by comparison with results obtained on SIRCUS. For this part of the calibration, relay optics were used to create a parallel 2.5 cm diameter beam. The radiation, under-filling the CCD field-of-view, was imaged onto a small region in the center of the CCD array. During the calibration, the radiant power in the beam was measured at each wavelength using reference detectors and an image subsequently acquired by the CCD. A 35 by 35 pixel area on the CCD was selected to give an averaged response. The data were subsequently corrected for the nonlinear response of the CCD and normalized to the radiant power in the beam, giving a relative responsivity of the CCD. To determine the absolute responsivity of the camera, the data were normalized to the SIRCUS results near 580 nm. Results are shown in Fig. 5 for the camera (a) with and (b) without the photopic filter attached.

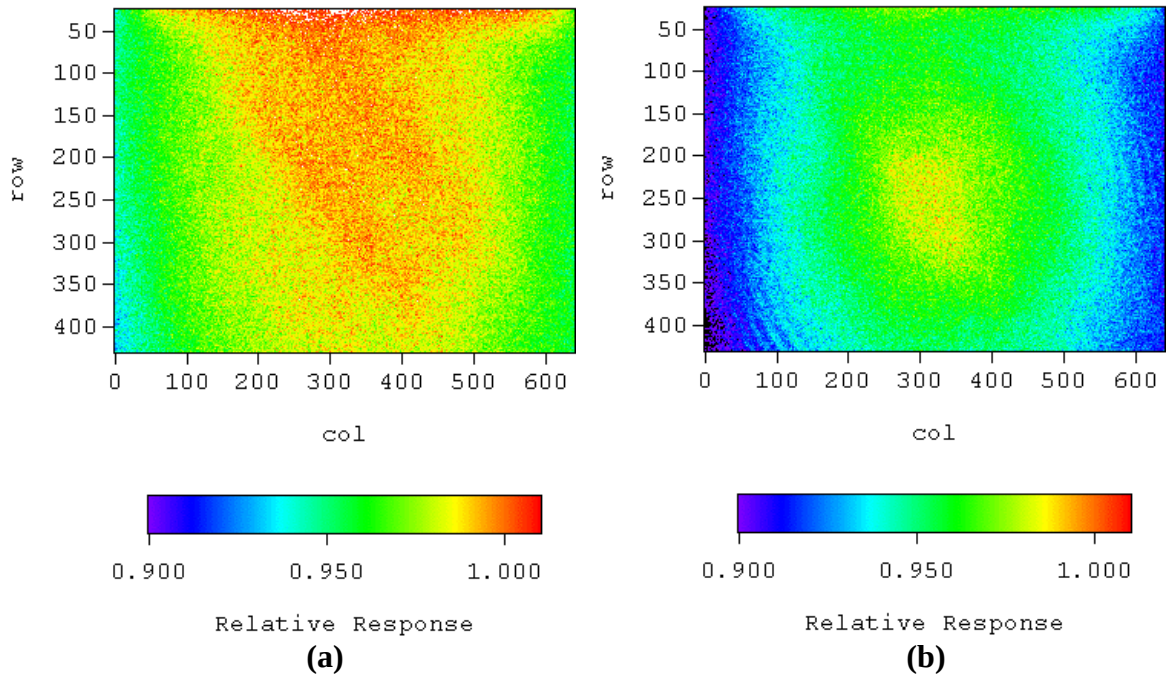

Fig. 4. Pixel-to-pixel uniformity (a)without and (b) with the photopic filter installed.

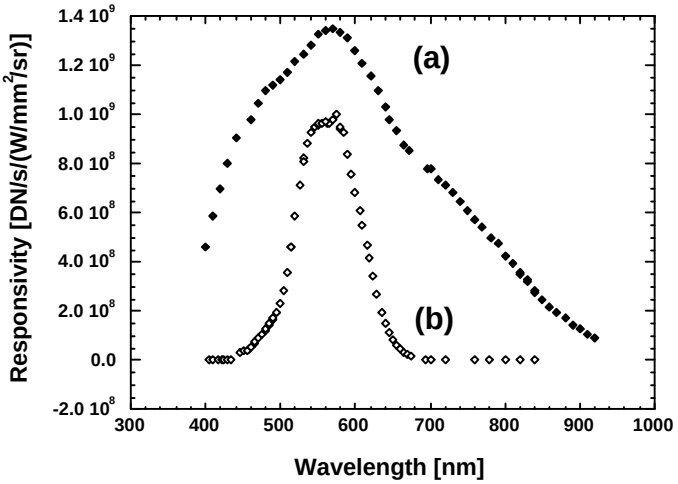

Fig. 5. CCD camera ASR (a) without and (b) with the photopic filter installed.

3.2. Uncertainty of camera radiance responsivity

Each component in the calibration chain contributes to the overall uncertainty in the radiance responsivity calibration. We estimated the contributions of all known components to the combined standard uncertainty in the CCD radiance responsivity calibration on SIRCUS. These contributions are listed in Table 1. We estimate that the relative combined standard uncertainty in the sphere radiance is 0.1 %, the uncertainty in the non-linear correction to the responsivity to be 1 %; the uncertainty in the exposure time correction to be 0.5 %; and the reproducibility, including short-term repeatability, alignment and focus, to be approximately 2 %. Taking the root-sum-square of the individual components, the relative combined standard uncertainty in the CCD radiance responsivity calibration is 2.3 % (coverage factor k=1). For imaging applications, there will be an additional uncertainty of approximately 1 % from the non-uniformity of the CCD.

Table 1. Relative combined standard uncertainty of the CCD radiance responsivity calibration on SIRCUS.

Component	Uncertainty [%]
Sphere Radiance (Monitor detector calibration)	0.1
Sphere Radiance Non-uniformity	0.25
CCD Non-linearity	1
Exposure time correction	0.5
Reproducibility	2
Relative Combined Std. Uncertainty	2.3

The radiant power distribution in the beam from the monochromator was highly non-uniform, leading to increased uncertainty in the calibration of the CCD, both because of the increased uncertainty in the reproducibility of the measurements, and also because of the increased uncertainty in the non-linearity correction of the averaged response. There was an additional uncertainty in the normalization of the response to the measurements on SIRCUS. Consequently, measurements using the lamp-monochromator had a relative combined standard uncertainty of approximately 4 %.

For measurements of photometric quantities, a source spectral radiance distribution is weighted by the $V(\lambda)$ function [7]. The photometric uncertainty is different than the above discussed radiometric responsivity measurement uncertainty and depends on how closely the response of the camera with the photopic filter approximates the $V(\lambda)$ function. For poor matches, the photometric uncertainty can be large and will depend on the source spectral distribution. There will be an additional uncertainty for imaging applications from the larger non-uniformity in the pixel-to-pixel response.

3.3 Microscope Calibration

The microscope consists of an objective lens and a 1024 by 1024 pixel cooled CCD array. It is used to determine x-ray phosphor efficiencies from scintillator crystals [8]. Imaging a scintillation region on a crystal is extremely advantageous because the radiation from scintillators is Lambertian and viewing the source distribution enables the determination of radiometric quantities with lower uncertainties. We measured the linearity, exposure time correction, pixel to pixel uniformity and the absolute spectral radiance responsivity of the microscope on SIRCUS. For these measurements, we used a 5 cm diameter ISS with a 2 mm aperture. The microscope, equipped with a 10X objective, was positioned in front of the ISS. Each pixel imaged the same region of the back wall of the ISS, resulting in minimal additional uncertainty in the calibration from any potential non-uniformity in the sphere exitance.

The CCD array had a 12-bit A/D converter, with 4095 DN corresponding to 90 % of the CCD full-well capacity. We first determined the exposure time and the non-linearity corrections in the response of the microscope; results are shown in Figs. 6 and 7, respectively. The exposure time correction was negligible for exposure times greater that 500 ms. For shorter exposure times, a correction — as large as 100 % for 10 ms exposure times — had to be applied. In many of these systems, there is a delay in opening and closing the shutter, leading to an exposure time that is slightly different than the nominal value. For this instrument, adding 10 ms to the nominal exposure time reduced the correction to the 5 % level for the shortest exposure times. The system response was linear for count rates larger than 100 DN. Offset variations and uncertainty in the determination of the background signal could contribute to the non-linear behavior at the smaller count rates. During the absolute radiometric calibration, the count rates were kept larger than 1000 DN and the exposure time was kept constant at 100 ms. This is easy to accomplish using a laser-based ISS; we merely adjust the power into the ISS at a given wavelength to achieve these goals.

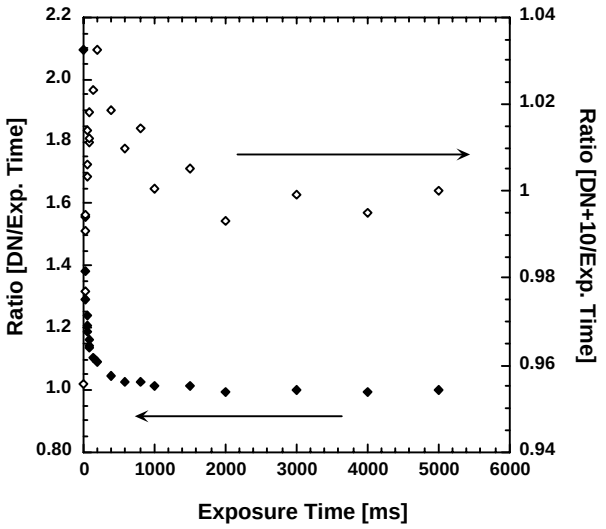

Fig. 6. Digital microscope exposure time correction.

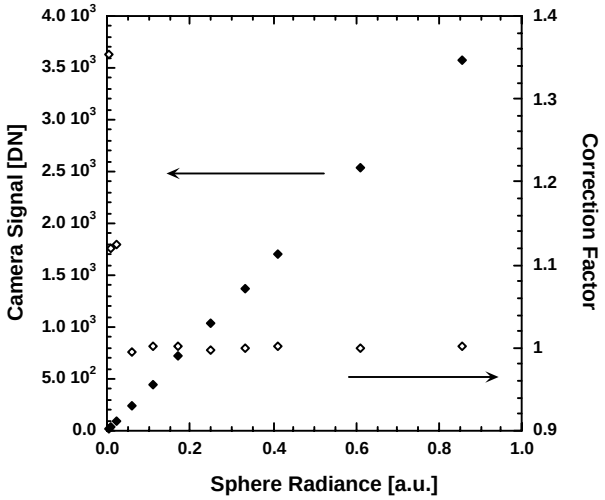

Fig. 7. Microscope response linearity.

The microscope response was uniform to with 0.2 % over the central 90 % of the CCD array; the ASR, averaged over the central 25 by 25 pixels, is shown in Fig. 8. Because of the smaller non-linear correction, the better pixel to pixel uniformity and the 12 bit digitization, we estimate the relative combined standard uncertainty in the microscope ASR measurement to be approximately 1 %.

3.4 Spectrograph Calibration

Spectrographs are typically calibrated for spectral radiance responsivity against broad-band sources such as lamp-illuminated integrating sphere sources (ISSs) and plaques. Stray light, wavelength errors, and lack of knowledge of the single pixel relative responsivity all give rise to increased uncertainties in the calibration and subsequent operation of these instruments. Many of these sources of calibration error can be greatly reduced or eliminated using tunable, monochromatic laser sources in place of conventional broad-band sources.

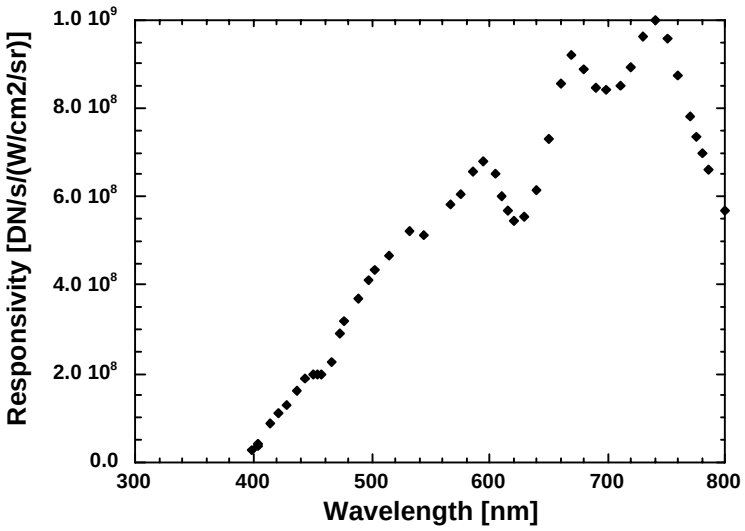

Fig. 8. ASR of digital microscope.

A dual-spectrograph radiometer was calibrated on SIRCUS for radiance responsivity over the spectral range from 400 nm to 850 nm. Details of the calibration are described elsewhere [4, 5]. In this instrument, radiation enters the spectrograph through an entrance slit, is dispersed using a grating, and imaged onto the CCD array using a mirror, as shown in Fig. 9. For excitation using monochromatic radiation, the image formed is a line reflecting the image of the entrance slit on the CCD (Fig. 10). Note that the image is spread out over several pixels in the horizontal (dispersion) direction, is not centered vertically on the CCD array, and shows a pronounced curvature (Fig. 11). By tuning the excitation wavelength, the image moves across the array and each pixel's ASR can be determined. In this work, we measured the responsivity of the averaged central 100 pixels in each column. Eq. 4 was modified to:

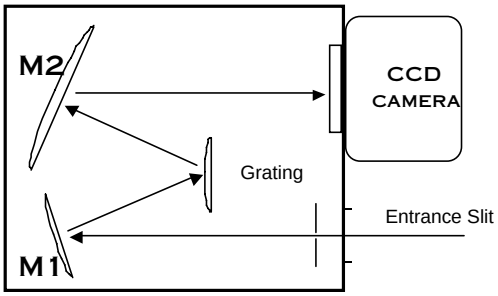

Fig. 9. Spectrograph optical layout.

$$R_i(\lambda_o) = S_i / L(\lambda_o), \qquad (5)$$

where *i* now refers to the particular column in the array. In Fig. 12, we show the absolute spectral responsivity, $R_i(\lambda)$, for columns 243 – 247 over the wavelength range from 735 nm to 750 nm. We measured a 0.8 nm separation between the maximum responsivity of adjacent pixels and nominal single pixel bandwidth of 2 nm. The curvature in the spectrograph image, Fig. 11 gave rise to the pronounced shoulder observed to shorter wavelength in the ASR. This shoulder in the single pixel ASR was attributed to the CCD not being located at the spectrograph image plane. We estimate the relative combined standard uncertainty in the calibration to be approximately 3 %. Note that the determination of each pixel's ASR is difficult to obtain using any technique other than the tunable-laser-based ISS approach developed on SIRCUS.

4. SUMMARY

We have developed a flexible, detector-based calibration facility using tunable laser sources and high accuracy reference standard detectors for the irradiance and radiance responsivity calibration of digital imaging systems. We have calibrated a number of instruments on this facility, and presented results for a digital camera, a digital microscope and a digital spectrograph. This approach has several advantages over conventional calibration techniques using broad-band sources, including uniform, monochromatic irradiance and radiance sources; lower wavelength uncertainty; no stray light contribution

to the signal; and the ability to determine each pixel's responsivity. Using this approach, uncertainties in the radiometric calibration of DIS's can be reduced by a factor of 2 or greater over conventional calibration techniques.

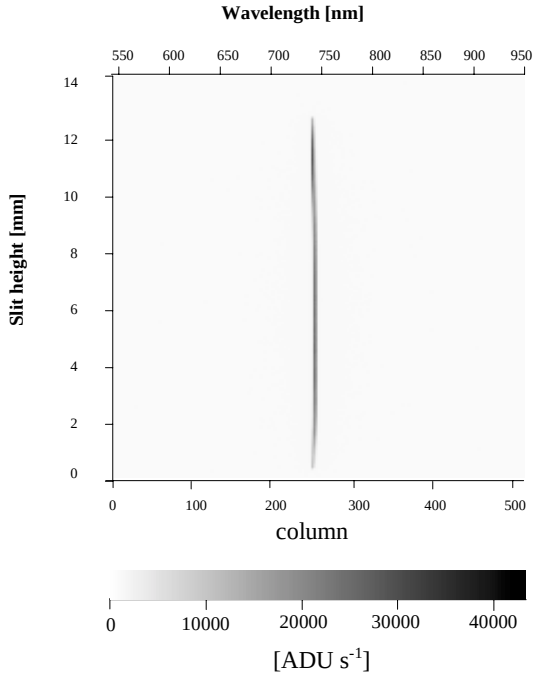

Fig. 10. Spectrograph image of ISS with 745 nm excitation.

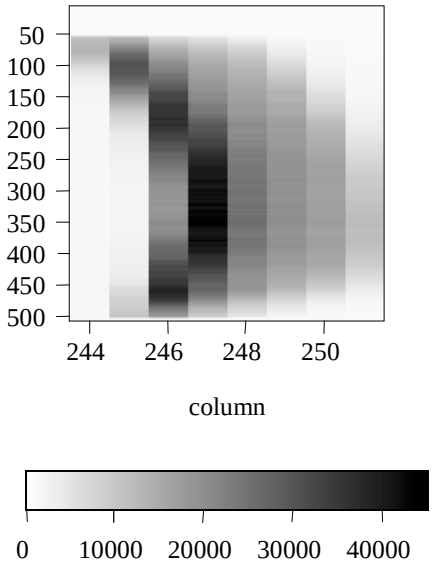

Fig. 11. Expanded view of spectrograph image of ISS with 745 nm excitation.

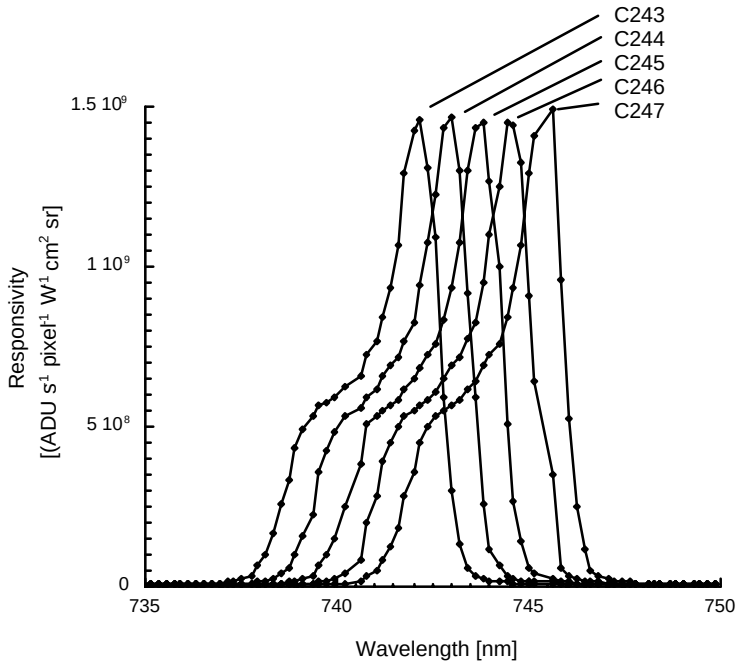

Fig. 12. Absolute spectral responsivity of columns 243 to 247.

5. ACKNOWLEDGMENTS

We would like to thank Carol Johnson for useful discussions and acknowledge support for this work by the U. S. Air Force Metrology under contract numbers 97-421 and 98-439.

6. REFERENCES

1 S. W. Brown, G. P. Eppeldauer, and K. R. Lykke, “NIST facility for spectral irradiance and radiance responsivity calibrations with uniform sources,” *Metrologia* 37, 579-582 (2000).

2 G.P. Eppeldauer and D.C. Lynch, "Opto-mechanical and electronic design of a tunnel-trap Si-radiometer," *J. Res. Natl. Inst. Stand. Technol*. (in press).

3 T. R. Gentile, J. M. Houston, J. E. Hardis, C. L. Cromer, and A. C. Parr, “National Institute of Standards and Technology high accuracy cryogenic radiometer,” *Appl. Opt*, 35, 1056-1068 (1996).

4 C. Habauzit, *et al*., “Radiometric characterization and absolute calibration of the Marine Optical System (MOS) bench unit,” *J. Atmos. and Ocean. Technol.*, to be submitted.

5 S. W. Brown, C. Habauzit, B. C. Johnson, and K. R. Lykke, “Tunable-laser-based calibration of a digital spectrograph,” *Appl. Opt*., to be submitted.

6 T. C. Larason, S. S. Bruce, and A. C. Parr, Spectroradiometric Detector Measurements, Natl. Inst. Stand. Technol. Spec. Publ. 250-41, U. S. Government Printing Office, Washington, DC, 1998.

7 Yoshihiro Ohno, Photometric Calibrations, Natl. Inst. Stand. Technol. Spec. Publ. 250-37, U. S. Government Printing Office, Washington, DC, 1997.

8 Steven Grantham, NIST, personal communication.